

This is the accepted manuscript (postprint) of the following article:

Majid Hosseinzadeh, Erfan Salahinejad, *Comparative analysis of electrodeposited Pt, Ru and Pt-Ru overlays for high-temperature oxidation protection*, Surface and Coatings Technology, 496 (2025) 131685.

<https://doi.org/10.1016/j.surfcoat.2024.131685>

Comparative Analysis of Electrodeposited Pt, Ru and Pt-Ru Overlays for High-Temperature Oxidation Protection

Majid Hosseinzadeh, Erfan Salahinejad*

Faculty of Materials Science and Engineering, K.N. Toosi University of Technology, Tehran, Iran

Abstract

Platinum (Pt) and ruthenium (Ru), both members of the platinum-group metals (PGMs), are renowned for their exceptional resistance to corrosion, oxidation, and high temperatures, making them promising candidates for advanced high-temperature applications. This study investigates the direct current (DC) electrodeposition of Pt, Ru, and a binary Pt-Ru alloy onto NiCoCrAlYTa-coated single-crystal superalloy CMSX-4, along with their vacuum annealing and respective effects on the isothermal oxidation behavior of the system at 1100 °C. All the electrodeposited overlays demonstrated substantial enhancement in oxidation resistance. However, Pt exhibited the highest protection efficiency, Ru the least, and the Pt-Ru alloy provided an intermediate level of performance. Microscopic and X-ray diffraction analyses revealed that the competitive formation of protective α -Al₂O₃ and spinel NiAl₂O₄ phases on the coated surfaces played a crucial role in determining the oxidation resistance, driven by atomic interactions between the elements in the NiCoCrAlYTa bond coat and the overlay metals. Despite Ru's relatively lower oxidation resistance compared to Pt, its significantly lower cost offers potential advantages in cost-sensitive, high-temperature applications. These

* Corresponding Author's Email Address: <salahinejad@kntu.ac.ir>

This is the accepted manuscript (postprint) of the following article:

Majid Hosseinzadeh, Erfan Salahinejad, *Comparative analysis of electrodeposited Pt, Ru and Pt-Ru overlays for high-temperature oxidation protection*, Surface and Coatings Technology, 496 (2025) 131685.

<https://doi.org/10.1016/j.surfcoat.2024.131685>

findings provide valuable insights into optimizing Pt-group metal coatings for durability in high-performance systems.

Keywords: Electroplating; Thermal barrier coatings (TBCs); MCrAlY; Chemical affinity; Diffusion; Enthalpy of mixing

1. Introduction

The aspiration of industries that use gas turbines, including power generation, oil and gas, marine, and aerospace, has always been to develop and use thermal barrier coatings (TBCs) that provide thermal insulation. In addition to TBCs that are primarily composed of ceramic materials, aluminide and MCrAlY (M stands for Ni, Co, or a combination of both) are extensively employed as bond coatings between the substrate and TBCs or as overlay coatings to protect the underlying metal from extreme heat. The deterioration of these metallic coatings, particularly due to oxidation, is a significant cause of the component failure [1-3]. The high-temperature resistance of these coatings is further enhanced through different strategies, including incorporation with platinum (Pt). Typically, Pt-modified aluminide diffusion coatings are used in certain industrial applications to offer protection efficiencies exceeding those of Pt-free aluminide coatings [4-6]. However, the exorbitant cost of Pt imposes significant constraints on its use, particularly for MCrAlY coatings that are already expensive, limiting its widespread applicability.

Ruthenium (Ru), another member of the Pt-group metals, exhibits thermodynamic properties similar to Pt, but costs only about a quarter of Pt. The increase in the resistance of aluminide and MCrAlY coatings to oxidation via Pt [7-9] and Ru [10-12] modifications has been distinctly reported. However, there are no comparative studies on the protection efficiency of these two additives, to our knowledge. In addition, the chemical and

This is the accepted manuscript (postprint) of the following article:

Majid Hosseinzadeh, Erfan Salahinejad, *Comparative analysis of electrodeposited Pt, Ru and Pt-Ru overlays for high-temperature oxidation protection*, Surface and Coatings Technology, 496 (2025) 131685.

<https://doi.org/10.1016/j.surfcoat.2024.131685>

electrochemical similarity of these two elements allows for the formation of their solid solution alloys across a wide range of composition, as indicated by their binary phase diagram [13]. While Pt-Ru alloys have been reported in catalytic applications such as direct methanol fuel cells [14-16], they have not been studied in high-temperature applications.

This work is focused on the comparative high-temperature oxidation characterization of MCrAlY coatings modified with Pt, Ru, and Pt-Ru overlays to explore the potential of Ru as an entire or partial replacement for expensive Pt in gas turbines. It is noteworthy that the deposition and subsequent effects of Ru overlays on both aluminide and MCrAlY coatings have not been reported before. In this study, as in most previous studies, electrodeposition is used to apply these layers due to the high melting points of the elements as well as high density results, equipment simplicity, and affordability associated with electrodeposition [17-19].

2. Experimental procedure

2.1. Sample preparation and characterization

A Ni-based single-crystal superalloy-CMSX-4 (nominal composition in wt%: 60.9Ni-9.5Co-6.5Ta-6.4Cr-6.3W-5.7Al-2.9Re-1.0Ti-0.6Mo-0.1Hf) was used as the substrate material, while disks of 10 mm in diameter and 1 mm in thickness were cut from rods. A NiCoCrAlYTa layer of almost 120 ± 10 μm in thickness was deposited on the substrate by a high velocity oxygen fuel (HVOF) technique from Amdry997 powder (Ni-23.0Co-20.0Cr-8.5Al-4.0Ta-0.6Y in wt%). HVOF deposition operation was conducted at a spraying distance of 255 mm, power feed rate of 50 g/min, O₂ flow of 800 L/min and N₂ flow of 15 L/min. Afterward, Pt, Ru, and Pt-Ru layers were electroplated on the NiCoCrAlYTa layer using electrolyte and electrodeposition conditions listed in Table 1, adapted from Refs. [19-21],

This is the accepted manuscript (postprint) of the following article:

Majid Hosseinzadeh, Erfan Salahinejad, *Comparative analysis of electrodeposited Pt, Ru and Pt-Ru overlays for high-temperature oxidation protection*, Surface and Coatings Technology, 496 (2025) 131685.

<https://doi.org/10.1016/j.surfcoat.2024.131685>

[19, 22, 23], and [24-26], respectively. The electroplating cell used had a fixed volume of 250 mL with a mixed metal oxide (MMO) anode whose surface area was three times larger than that of the cathode. The distance between the cathode and anode was kept constant at 4 cm throughout the electroplating process. To maintain a stable pH of the electrolyte, HCl and NaOH were used. The coated samples were vacuum-annealed at 1080 °C for 6 h.

Table 1. Bath composition and electroplating parameters for depositing Pt, Ru, and Pt-Ru coatings.

Compositions/Parameters	Pt coating	Ru coating	Pt-Ru coating
Pt(NH ₃) ₂ (NO ₂) ₂ (mol/L)	0.03	-	0.03
Na ₂ CO ₃ (mol/L)	0.15	-	0.15
NaCH ₃ COO (mol/L)	0.12	-	0.12
RuCl ₃ (mol/L)	-	0.02	0.02
HCl (mol/L)	-	0.30	0.30
NaCl (mol/L)	-	0.03	0.03
Current density (A/dm ²)	0.5	2	3
Temperature (°C)	90	70	75
Solution pH	11	1	3
Time (min)	180	60	90

The top and cross section of the coatings were characterized using field-emission electron microscopy (FESEM, MIRA3, TESCAN) equipped with energy dispersive X-ray spectrometry (EDS). Reference lines for EDS line scans were selected from regions of the coatings that visually appeared representative of the overall morphology and had thicknesses close to the calculated average coating thickness. The thickness is expressed as the mean ± standard deviation across three repeated samples, with measurements obtained from three regions per sample. The coatings were also tested for bonding strength according to the

This is the accepted manuscript (postprint) of the following article:

Majid Hosseinzadeh, Erfan Salahinejad, *Comparative analysis of electrodeposited Pt, Ru and Pt-Ru overlays for high-temperature oxidation protection*, Surface and Coatings Technology, 496 (2025) 131685.

<https://doi.org/10.1016/j.surfcoat.2024.131685>

ASTM C633 standard [27]. The method involved fastening the coated samples to an uncoated sample using SW 2214 epoxy adhesive (3M Scotch-weld, bond strength~70 MPa), which was applied at 150 °C for 2 h to ensure a strong bond. The samples were then subjected to a tensile load at a rate of 5 mm/min until fracture, and the corresponding fracture stress was recorded with five repetitions.

2.2. Analysis of oxidation protection

Isothermal oxidation tests were carried out in a muffle furnace under static air conditions at 1100 °C up to 100 h. Mass changes of the oxidized samples together with an alumina crucible were measured at regular intervals using an electronic balance with the sensitivity of 10^{-4} g at three repetitions. In addition, FESEM-EDS and X-ray diffraction (XRD) analyses were conducted to explore the surface morphology, composition, and phase of the oxidated coatings.

3. Results and discussion

3.1. Structural and bonding characterization of the annealed samples

The secondary electron (SE) surface morphology and EDS spectra of the electrodeposited, annealed Pt, Ru, and Pt-Ru coatings are illustrated in Fig. 1. As can be observed, the Pt coating exhibits a globular structure in agreement with Refs. [28-30], while the Ru coating has a cauliflower structure that is compatible with Refs. [22] and the Pt-Ru coating is characterized by a dendritic growth mode that aligns with Ref. [31]. In general, the globular structure results from uniform nucleation across the substrate, leading to consistent growth in all directions. This occurs under charge-transfer controlled deposition, where a high concentration of ions and low overpotential promote stable, compact grain formation as

This is the accepted manuscript (postprint) of the following article:

Majid Hosseinzadeh, Erfan Salahinejad, *Comparative analysis of electrodeposited Pt, Ru and Pt-Ru overlays for high-temperature oxidation protection*, Surface and Coatings Technology, 496 (2025) 131685.

<https://doi.org/10.1016/j.surfcoat.2024.131685>

atoms minimize surface energy. This morphology is characteristic of elements that exhibit high deposition efficiency, high reduction potential, and are supplied in sufficient concentrations [32-34]. In contrast, the cauliflower structure arises from diffusion-controlled growth, where the rate of nucleation exceeds the rate of diffusion, resulting in uneven growth and the formation of a more disordered structure [32, 34, 35]. The dendritic morphology of the Pt-Ru coating arises from the simultaneous co-deposition of Pt and Ru, driven by their differing deposition mechanisms. Pt, with charge-transfer-controlled deposition, forms the core structure through compact nucleation due to its higher reduction potential. Ru, governed by diffusion-controlled deposition, contributes to branching by nucleating on the Pt framework. This interplay of mechanisms is characteristic of dendritic structures formed through co-electrodeposition [36-39].

This is the accepted manuscript (postprint) of the following article:

Majid Hosseinzadeh, Erfan Salahinejad, *Comparative analysis of electrodeposited Pt, Ru and Pt-Ru overlays for high-temperature oxidation protection*, Surface and Coatings Technology, 496 (2025) 131685.

<https://doi.org/10.1016/j.surfcoat.2024.131685>

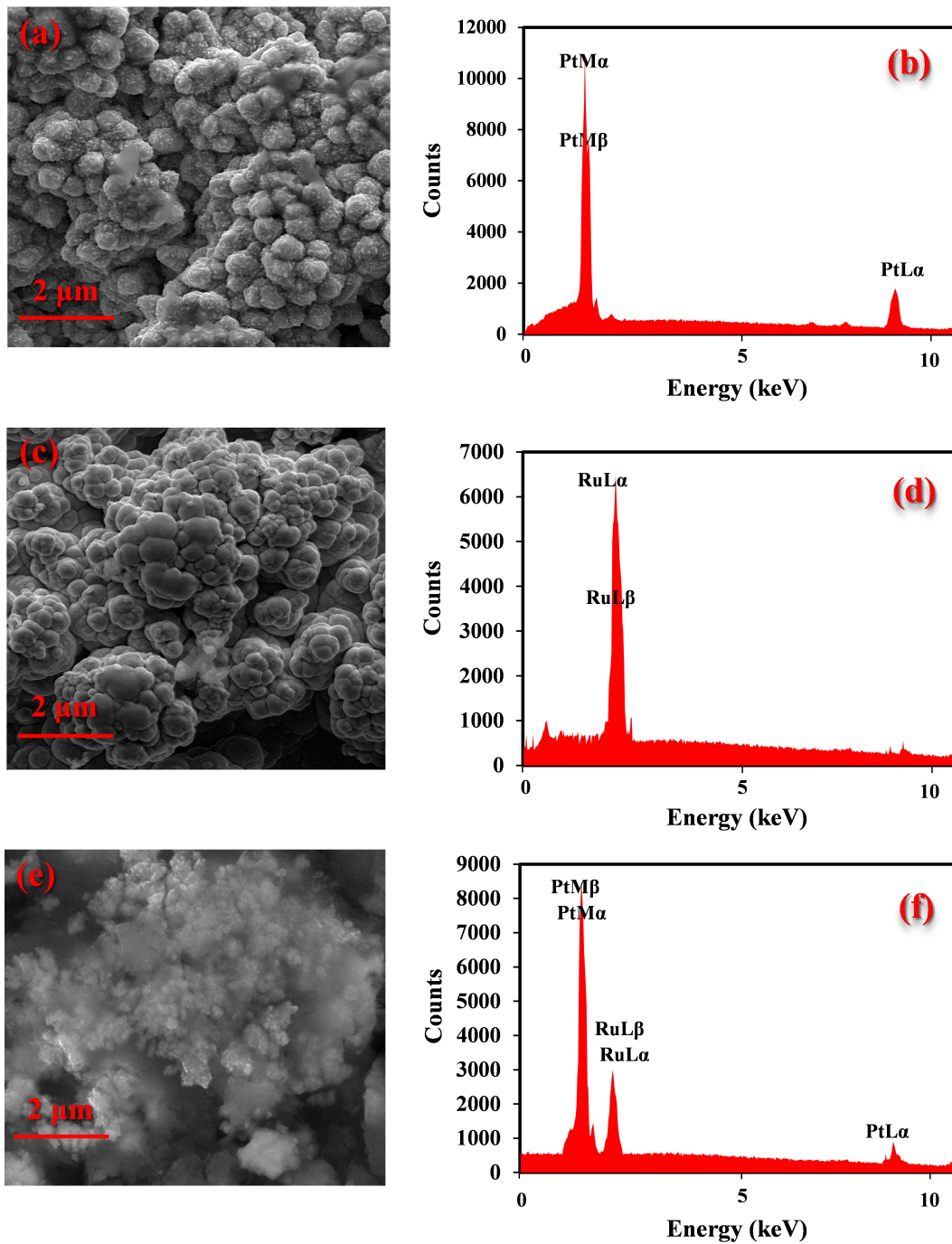


Fig. 1. SE micrographs and EDS spectra of the electrodeposited pure Pt (a, b), pure Ru (c, d), and Pt-Ru alloy (e, f) coatings.

This is the accepted manuscript (postprint) of the following article:

Majid Hosseinzadeh, Erfan Salahinejad, *Comparative analysis of electrodeposited Pt, Ru and Pt-Ru overlays for high-temperature oxidation protection*, Surface and Coatings Technology, 496 (2025) 131685.

<https://doi.org/10.1016/j.surfcoat.2024.131685>

The chemical composition of the coatings was validated by the EDS analysis, with 66Pt-34Ru (wt%) obtained for the alloy deposit, while the loaded weight ratio of Pt to Ru was 60/40 to provide a single-phase platinum-rich alloy based on the binary phase diagram [40]. However, the actual composition of the alloy deposited by electroplating is determined by not only the nominal ionic composition of the bath, but also the differential electrodeposition rates of elements [25, 41]. Typically, Pt, with its higher reduction potential, tends to deposit more rapidly in diffusion-limited conditions, while Ru, with a lower reduction potential, deposits more slowly under kinetically-limited conditions [39].

The cross-sectional backscattered electron (BSE) images, EDS linear scans, and elemental maps taken from the samples are presented in Figs. 2 and 3. The Pt, Ru, and Pt-Ru coatings exhibit thicknesses of 6.0 ± 0.5 , 5.0 ± 1.0 , and 5 ± 0.5 μm , respectively. These measurements are consistent with the thicknesses predicted by Faradaic thickness calculations [42], indicating that the deposition processes were well-controlled. The standard deviations in thickness aligns with the morphological structures observed in Fig. 1, influencing the uniformity of the coating thickness. Globular structures, as seen in the Pt coating, typically result in more uniform coatings with lower standard deviations. In contrast, more complex morphologies, such as the cauliflower-like structure of the Ru coating and the dendritic growth observed in the Pt-Ru coating, contribute to greater variability in the coating thickness. This relationship highlights how the morphology influences the uniformity of the coating thickness, with more irregular structures leading to increased thickness variability.

This is the accepted manuscript (postprint) of the following article:

Majid Hosseinzadeh, Erfan Salahinejad, *Comparative analysis of electrodeposited Pt, Ru and Pt-Ru overlays for high-temperature oxidation protection*, Surface and Coatings Technology, 496 (2025) 131685.

<https://doi.org/10.1016/j.surfcoat.2024.131685>

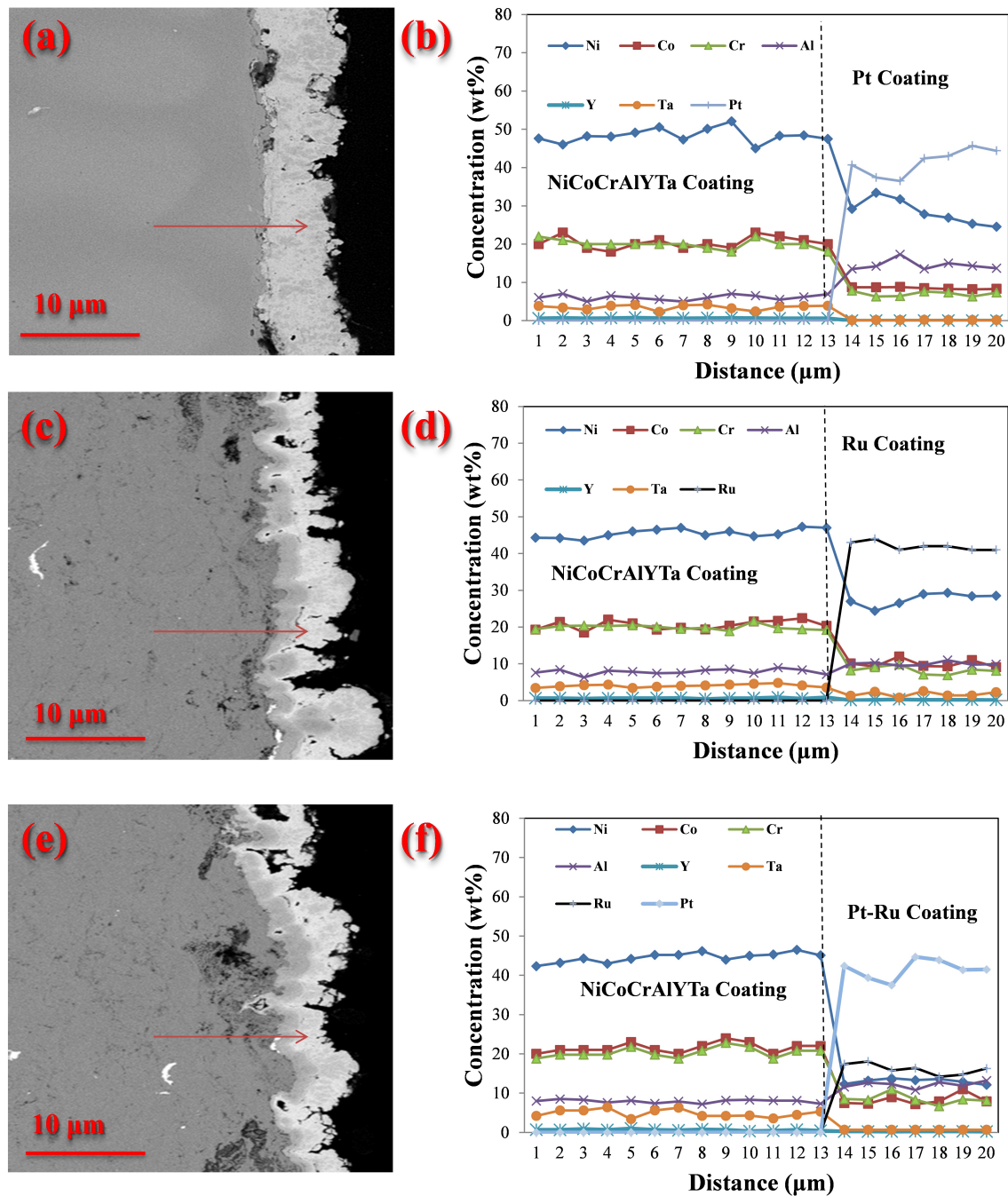


Fig. 2. BSE cross-sectional images and corresponding EDS line scans for the Pt (a, b), Ru (c, d), and Pt-Ru (e, f) coatings.

This is the accepted manuscript (postprint) of the following article:

Majid Hosseinzadeh, Erfan Salahinejad, *Comparative analysis of electrodeposited Pt, Ru and Pt-Ru overlays for high-temperature oxidation protection*, Surface and Coatings Technology, 496 (2025) 131685.

<https://doi.org/10.1016/j.surfcoat.2024.131685>

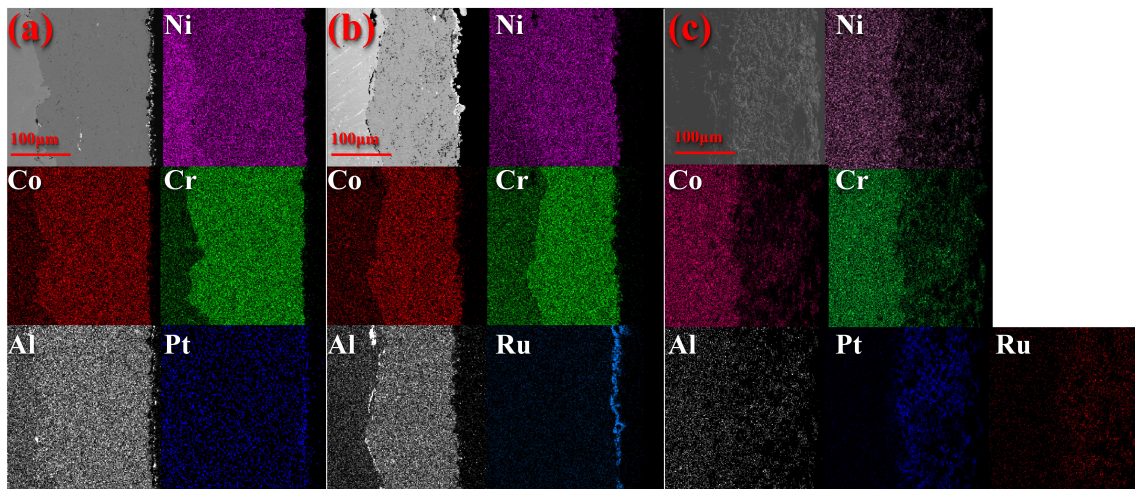


Fig. 3. BSE cross-sectional images and EDS elemental distribution maps for the Pt (a), Ru (b), and Pt-Ru (c) coatings.

The EDS linear scans and elemental maps confirm the relatively uniform distribution of Pt and Ru at the microscale within the coatings. No significant interdiffusion of Pt and Ru into the underlay coat was detected. However, certain constituent elements of the bond coat have outward diffused into the Pt-group overlays, with surface concentrations listed in Table 2. As observed, the surface concentrations of Ni, Co, Cr, and Al on the Pt overlay are higher than those on the Ru coating, while the concentrations of Y and Ta on the Ru coating are higher compared to the Pt overlay. The concentrations on the alloy overlay fall between those observed on the elemental coatings.

Table 2. EDS-extracted concentration of the bond coat elements on the surface of the electrodeposited overlays

Coatings	Elements					
	Ni	Co	Cr	Al	Y	Ta
Pt	33.4	8.6	9.1	14.1	0	0.2

This is the accepted manuscript (postprint) of the following article:

Majid Hosseinzadeh, Erfan Salahinejad, *Comparative analysis of electrodeposited Pt, Ru and Pt-Ru overlays for high-temperature oxidation protection*, Surface and Coatings Technology, 496 (2025) 131685.

<https://doi.org/10.1016/j.surfcoat.2024.131685>

Ru	31.5	7.8	8.3	5.5	0.2	1.7
Pt-Ru	32.1	8.2	8.6	8.4	0	0.7

The distribution of elements in diffusion couples is generally determined by both thermodynamic and kinetic factors in terms of interactions and diffusivities of the elements involved, respectively. The enthalpy of mixing of a pair is closely related to their affinity, which describes how strongly they interact with each other when mixed. A positive enthalpy of mixing generally indicates that phase separation or limited solubility is energetically more favorable than the formation of a stable mixed phase or interdiffusion. A moderately negative enthalpy of mixing usually indicates the formation of a solid solution or interdiffusion, while highly negative enthalpy of mixing typically suggests the formation of new phases like intermetallic compounds with slower diffusivity due to the more rigid and ordered lattice structure [43, 44]. Table 3 lists the enthalpy of mixing for the elements in the bond coat when combined with Pt and Ru. To explain the interdiffusion of Pt and Ru in the bond coat, it is indeed practical to focus primarily on interactions between Pt and Ru with Ni and Co as they are the major components in the bond coat alloy (Ni-23.0Co-20.0Cr-8.5Al-4.0Ta-0.6Y in wt%). The small negative enthalpy of mixing for these pairs indicates a limited affinity between the elements, resulting in the restricted interdiffusion of Pt and Ru into the bond coat. In contrast, Ni and Co exhibit higher interdiffusion into the overlays, as their smaller atomic sizes facilitate greater diffusivity compared to Pt and Ru. The moderately negative enthalpy of mixing for Cr and Al with Pt and Ru explains their interdiffusion into the overlay coatings, with a higher concentration observed in the Pt coating due to its greater affinity for these elements. The moderately negative enthalpy of mixing for Y and Ta with Ru explains their interdiffusion into the Ru overlay, while the highly negative enthalpy of mixing for Y

This is the accepted manuscript (postprint) of the following article:

Majid Hosseinzadeh, Erfan Salahinejad, *Comparative analysis of electrodeposited Pt, Ru and Pt-Ru overlays for high-temperature oxidation protection*, Surface and Coatings Technology, 496 (2025) 131685.

<https://doi.org/10.1016/j.surfcoat.2024.131685>

and Ta with Pt is responsible for their blocked interdiffusion into the Pt overlay. This is supported by their binary phase diagrams, which demonstrate the low solubility of Y and Ta in Pt, as well as the formation of multiple intermetallic compounds between these pairs [45].

Table 3. Enthalpy of mixing of the elements existing in the bond coat with Pt and Ru [43, 44]

		ΔH_{mix} (kJ/mol)					
		Ni	Co	Cr	Al	Y	Ta
Pt		-5	-7	-24	-44	-83	-66
Ru		0	-1	-12	-21	-34	-39

The adhesion strength of the Pt, Ru, and Pt-Ru coatings was measured to be 43.2 ± 3.5 , 39.1 ± 4.5 , and 40.3 ± 4.0 MPa, respectively. While the variations in the bonding strength of the coatings are minimal, they can be explained by considering the observed surface morphology (Fig. 1) and the interdiffusion of the atoms between the electrodeposited coatings and underlying bond coat (Fig. 2). Surface morphology influences bonding strength by affecting the uniformity and compactness of the coating-substrate interface [46, 47]. Typically, a more uniform and compact morphology, such as the Pt's globular structure, enhances bonding strength, while complex, irregular morphologies, like Ru's cauliflower structure, can weaken it. Pt-Ru, exhibiting dendritic growth, combines the characteristics of both materials, resulting in intermediate bonding strength. The bonding strength can also be influenced by thermodynamic and kinetic interactions between the elements in the layers [48-50]. Pt shows stronger affinity and interdiffusion with the principal elements of the underlying coating, which is favorable for adhesion, while the Ru's lower affinity and diffusion could limit its ability to bond effectively to the substrate. The moderate behavior of

This is the accepted manuscript (postprint) of the following article:

Majid Hosseinzadeh, Erfan Salahinejad, *Comparative analysis of electrodeposited Pt, Ru and Pt-Ru overlays for high-temperature oxidation protection*, Surface and Coatings Technology, 496 (2025) 131685.

<https://doi.org/10.1016/j.surfcoat.2024.131685>

Pt-Ru likely leads to an intermediate bonding strength due to the varied behaviors of Pt and Ru within the coating.

3.2. Isothermal oxidation characterization of the samples

The 1100 °C isothermal oxidation kinetic curves for the samples are illustrated in Fig. 4. All the samples exhibit a sharp weight gain within the first hour of exposure due to the rapid formation of oxide scales, a common behavior during high-temperature oxidation where the formation of an oxide layer protects the underlying metal from further oxidation [51, 52]. As can be also seen, the employment of the electrodeposited overlayers has significantly improved oxidization resistance when compared with the control sample (bare NiCoCrAlYTa). Comparing the electrodeposition-coated samples, the Pt-coated sample exhibits the least weight gain, the Ru-coated sample the highest, and the Pt/Ru-coated sample an intermediate amount over the entire oxidation period. This suggests that Pt promotes the formation of a more stable and continuous oxide layer compared to Ru, which leads to better protection of the underlying metal substrate.

This is the accepted manuscript (postprint) of the following article:

Majid Hosseinzadeh, Erfan Salahinejad, *Comparative analysis of electrodeposited Pt, Ru and Pt-Ru overlays for high-temperature oxidation protection*, Surface and Coatings Technology, 496 (2025) 131685.

<https://doi.org/10.1016/j.surfcoat.2024.131685>

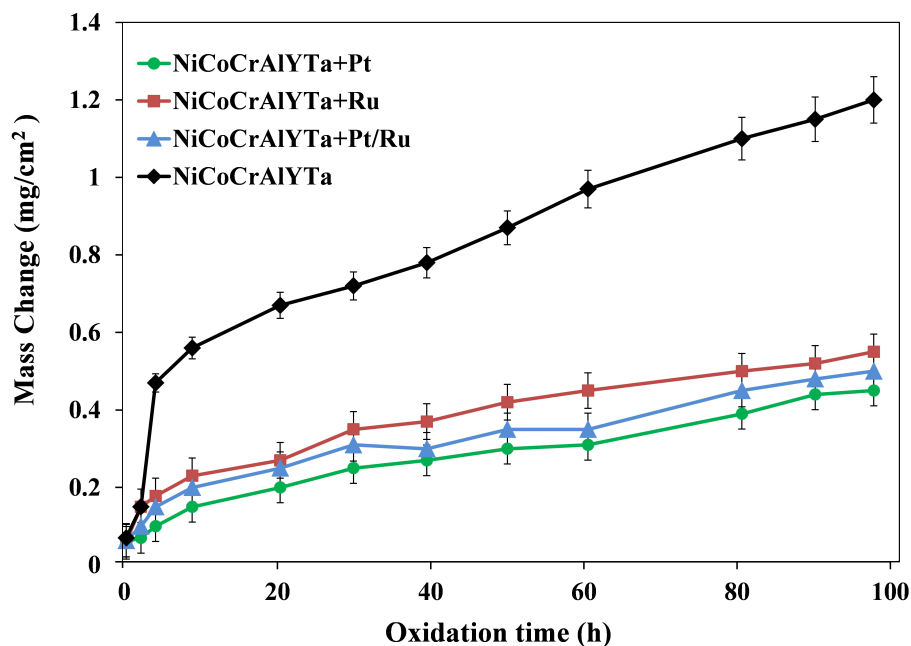


Fig. 4. Isothermal oxidation curves of the NiCoCrAlYT a+Pt, NiCoCrAlYT a+Ru, and NiCoCrAlYT a+Pt/Ru samples.

Fig. 5 depicts the XRD patterns of the samples after isothermal oxidation at 1100 °C for 100 h. Based on the peak analysis, the dominant oxide scale formed on all the coating surfaces is Al₂O₃ with weak diffraction signals from the spinel NiAl₂O₄ phase. Also, the Pt, Ru, and Pt/Ru-coated samples contain γ -Ni(Pt) / γ' -(Ni,Pt)₃Al, γ -Ni(Ru) / γ' -(Ni,Ru)₃Al, and γ -Ni(Pt,Ru) / γ' -(Ni,Pt,Ru)₃Al, respectively. The relative number and intensity of the Al₂O₃ peaks rank as Pt > Pt-Ru > Ru, which aligns well with the elemental distribution in the overlay coatings (Fig. 2) and the oxidation resistance ranking (Fig. 4), as Al₂O₃ serves as the essential phase providing oxidation protection in the thermally-grown oxide (TGO) layer [7, 53, 54]. In contrast, diffraction signals for the spinel NiAl₂O₄ phase rank as Ru > Pt-Ru > Pt, which is in consistent with the observed oxidation behavior, as this phase deteriorates the

This is the accepted manuscript (postprint) of the following article:

Majid Hosseinzadeh, Erfan Salahinejad, *Comparative analysis of electrodeposited Pt, Ru and Pt-Ru overlays for high-temperature oxidation protection*, Surface and Coatings Technology, 496 (2025) 131685.

<https://doi.org/10.1016/j.surfcoat.2024.131685>

oxidation protection of the TGO due to a higher growth rate compared to α -Al₂O₃ [52, 55, 56].

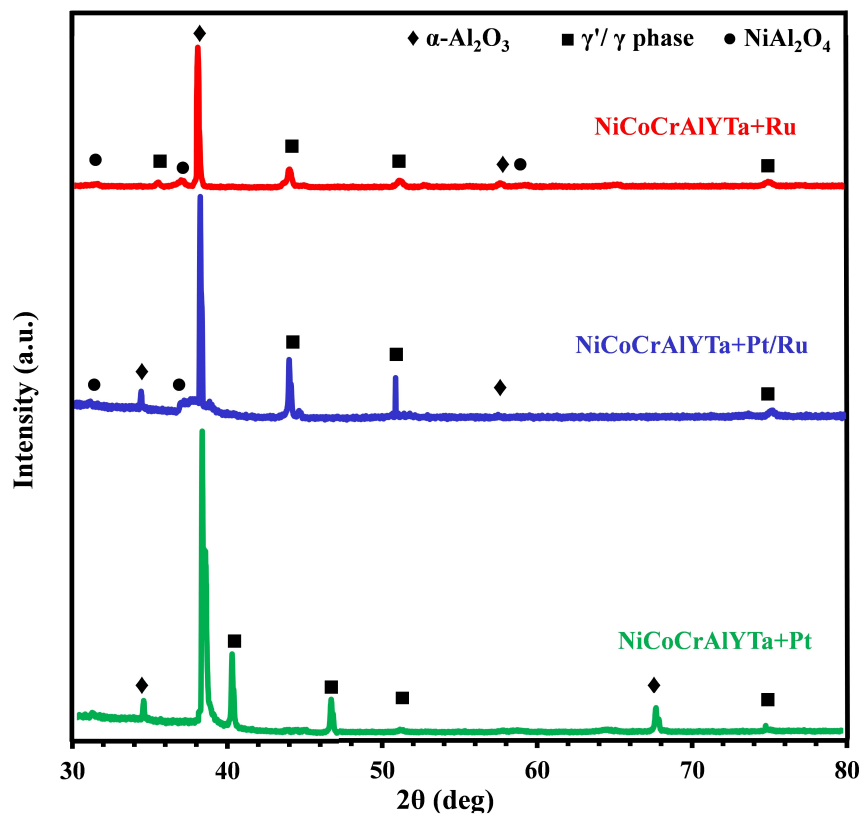


Fig. 5. XRD patterns of the NiCoCrAlYTa+Pt, NiCoCrAlYTa+Ru, and NiCoCrAlYTa+Pt/Ru samples.

4. Conclusions

This study demonstrated that the electrodeposition of Pt, Ru, and Pt-Ru onto NiCoCrAlTaY-coated CMSX-4 superalloy, followed by vacuum annealing at 1080 °C for 6 h, significantly improves oxidation resistance at 1100 °C. Among the three coatings, Pt provided the highest oxidation protection, followed by the Pt-Ru alloy, with Ru offering the least protection. Despite Ru's lower performance in terms of oxidation resistance, its cost-effectiveness and high-temperature properties offer potential for replacing or supplementing

This is the accepted manuscript (postprint) of the following article:

Majid Hosseinzadeh, Erfan Salahinejad, *Comparative analysis of electrodeposited Pt, Ru and Pt-Ru overlays for high-temperature oxidation protection*, Surface and Coatings Technology, 496 (2025) 131685.

<https://doi.org/10.1016/j.surfcoat.2024.131685>

Pt in cost-sensitive applications. These findings suggest that the Pt-Ru alloy could serve as a viable compromise between performance and cost, providing an intermediate solution for advanced high-temperature systems. Future work may focus on optimizing the alloy composition to further balance these factors for industrial applications.

References

1. Padture, N.P., M. Gell, and E.H. Jordan, *Thermal barrier coatings for gas-turbine engine applications*. Science, 2002. **296**(5566): p. 280-284.
2. Gao, W., *Developments in high temperature corrosion and protection of materials*. 2008: Elsevier.
3. Vaßen, R., et al., *Overview on advanced thermal barrier coatings*. Surface and Coatings Technology, 2010. **205**(4): p. 938-942.
4. Chen, M., et al., *Characterization and modeling of a martensitic transformation in a platinum modified diffusion aluminide bond coat for thermal barrier coatings*. Acta Materialia, 2003. **51**(14): p. 4279-4294.
5. Yu, C., et al., *High-temperature performance of (Ni, Pt) Al coatings on second-generation Ni-base single-crystal superalloy at 1100 C: Effect of excess S impurities*. Corrosion Science, 2019. **159**: p. 108115.
6. Liu, H., et al., *Improving cyclic oxidation resistance of Ni3Al-based single crystal superalloy with low-diffusion platinum-modified aluminide coating*. Journal of Materials Science & Technology, 2020. **54**: p. 132-143.
7. Put, A.V., et al., *Effect of modification by Pt and manufacturing processes on the microstructure of two NiCoCrAlYTa bond coatings intended for thermal barrier system applications*. Surface and Coatings Technology, 2010. **205**(3): p. 717-727.
8. Das, D., *Microstructure and high temperature oxidation behavior of Pt-modified aluminide bond coats on Ni-base superalloys*. Progress in Materials Science, 2013. **58**(2): p. 151-182.
9. Yang, Y., et al., *Modification of NiCoCrAlY with Pt: Part I. Effect of Pt depositing location and cyclic oxidation performance*. Journal of materials science & technology, 2019. **35**(3): p. 341-349.
10. Juarez, F., et al., *Chemical vapor deposition of ruthenium on NiCoCrAlYTa powders followed by thermal oxidation of the sintered coupons*. Surface and Coatings Technology, 2003. **163**: p. 44-49.
11. Tryon, B., et al., *Ruthenium-containing bond coats for thermal barrier coating systems*. JoM, 2006. **58**: p. 53-59.
12. Bai, B., et al., *Cyclic oxidation and interdiffusion behavior of a NiAlDy/RuNiAl coating on a Ni-based single crystal superalloy*. Corrosion Science, 2011. **53**(9): p. 2721-2727.
13. Okamoto, H. and T. Massalski, *Binary alloy phase diagrams*. ASM International, Materials Park, OH, USA, 1990. **12**.

This is the accepted manuscript (postprint) of the following article:

Majid Hosseinzadeh, Erfan Salahinejad, *Comparative analysis of electrodeposited Pt, Ru and Pt-Ru overlays for high-temperature oxidation protection*, Surface and Coatings Technology, 496 (2025) 131685.

<https://doi.org/10.1016/j.surfcoat.2024.131685>

14. Bauer, A., E.L. Gyenge, and C.W. Oloman, *Electrodeposition of Pt–Ru nanoparticles on fibrous carbon substrates in the presence of nonionic surfactant: application for methanol oxidation*. *Electrochimica acta*, 2006. **51**(25): p. 5356-5364.
15. Jow, J.-J., et al., *Co-electrodeposition of Pt–Ru electrocatalysts in electrolytes with varying compositions by a double-potential pulse method for the oxidation of MeOH and CO*. *International Journal of Hydrogen Energy*, 2009. **34**(2): p. 665-671.
16. Sun, Y., et al., *Robust PtRu catalyst regulated via cyclic electrodeposition for electrochemical production of cyclohexanol*. *Journal of Catalysis*, 2024. **429**: p. 115219.
17. Sieben, J.M., M.M.E. Duarte, and C.E. Mayer, *Supported Pt and Pt–Ru catalysts prepared by potentiostatic electrodeposition for methanol electrooxidation*. *Journal of Applied Electrochemistry*, 2008. **38**: p. 483-490.
18. Coutanceau, C., et al., *Preparation of Pt–Ru bimetallic anodes by galvanostatic pulse electrodeposition: characterization and application to the direct methanol fuel cell*. *Journal of applied electrochemistry*, 2004. **34**: p. 61-66.
19. Rao, C.R. and D. Trivedi, *Chemical and electrochemical depositions of platinum group metals and their applications*. *Coordination Chemistry Reviews*, 2005. **249**(5-6): p. 613-631.
20. Li, S., et al., *Co-doping effect of Hf and Y on improving cyclic oxidation behavior of (Ni, Pt) Al coating at 1150° C*. *Corrosion Science*, 2021. **178**: p. 109093.
21. Reid, F.H., *Electrodeposition of the platinum-group metals*. *Metallurgical Reviews*, 1963. **8**(1): p. 167-211.
22. Oppedisano, D.K., et al., *Ruthenium electrodeposition from aqueous solution at high cathodic overpotential*. *Journal of The Electrochemical Society*, 2014. **161**(10): p. D489.
23. Kutyla, D., et al., *Investigation of ruthenium thin layers electrodeposition process under galvanostatic conditions from chloride solutions*. *Russian Journal of Electrochemistry*, 2020. **56**: p. 214-221.
24. He, Z., et al., *Electrodeposition of Pt–Ru nanoparticles on carbon nanotubes and their electrocatalytic properties for methanol electrooxidation*. *Diamond and Related Materials*, 2004. **13**(10): p. 1764-1770.
25. Li, C., et al., *Electrodeposition of Pt–Ru alloy electrocatalysts for direct methanol fuel cell*. *International Journal of Electrochemical Science*, 2017. **12**(3): p. 2485-2494.
26. Colmati Jr, F., et al., *Carbon monoxide oxidation on Pt-Ru electrocatalysts supported on high surface area carbon*. *Journal of the Brazilian Chemical Society*, 2002. **13**: p. 474-482.
27. Testing, A.S.f. and Materials. *Standard test method for adhesion or cohesion strength of thermal spray coatings*. 2001. ASTM West Conshohocken (PA).
28. Plyasova, L., et al., *Electrodeposited platinum revisited: Tuning nanostructure via the deposition potential*. *Electrochimica Acta*, 2006. **51**(21): p. 4477-4488.
29. Zhang, H., et al., *Effect of deposition potential on the structure and electrocatalytic behavior of Pt micro/nanoparticles*. *International Journal of Hydrogen Energy*, 2011. **36**(23): p. 15052-15059.
30. Yu, C., et al., *High-temperature performance of Pt-modified Ni-20Co-28Cr-10Al-0.5 Y coating: Formation mechanism of Pt-rich overlayer and its effect on thermally grown oxide failure*. *Surface and Coatings Technology*, 2023. **461**: p. 129422.

This is the accepted manuscript (postprint) of the following article:

Majid Hosseinzadeh, Erfan Salahinejad, *Comparative analysis of electrodeposited Pt, Ru and Pt-Ru overlays for high-temperature oxidation protection*, Surface and Coatings Technology, 496 (2025) 131685.

<https://doi.org/10.1016/j.surfcoat.2024.131685>

31. Lu, X., et al., *Electrochemical deposition of Pt–Ru on diamond electrodes for the electrooxidation of methanol*. Journal of electroanalytical chemistry, 2011. **654**(1-2): p. 38-43.
32. Hyde, M.E. and R.G. Compton, *A review of the analysis of multiple nucleation with diffusion controlled growth*. Journal of Electroanalytical Chemistry, 2003. **549**: p. 1-12.
33. Lu, G. and G. Zangari, *Electrodeposition of platinum on highly oriented pyrolytic graphite. Part I: electrochemical characterization*. The Journal of Physical Chemistry B, 2005. **109**(16): p. 7998-8007.
34. Paunovic, M., *Fundamentals of Electrochemical Deposition*. Joh Wiley & Sons, 2006.
35. Hacıismailoglu, M. and M. Alper, *Effect of electrolyte pH and Cu concentration on microstructure of electrodeposited Ni–Cu alloy films*. Surface and Coatings Technology, 2011. **206**(6): p. 1430-1438.
36. Muthukumar, V. and R. Chetty, *Morphological transformation of electrodeposited Pt and its electrocatalytic activity towards direct formic acid fuel cells*. Journal of Applied Electrochemistry, 2017. **47**: p. 735-745.
37. Goranova, D., G. Avdeev, and R. Rashkov, *Electrodeposition and characterization of Ni–Cu alloys*. Surface and Coatings Technology, 2014. **240**: p. 204-210.
38. Lee, J.M., et al., *Creation of microstructured surfaces using Cu–Ni composite electrodeposition and their application to superhydrophobic surfaces*. Applied Surface Science, 2014. **289**: p. 14-20.
39. Goranova, D., et al., *Electrodeposition of Ni–Cu alloys at high current densities: details of the elements distribution*. Journal of Materials Science, 2016. **51**: p. 8663-8673.
40. Massalski, T. and P. Subramanian, *Hf (Hafnium) Binary Alloy Phase Diagrams*. ASM international Cleveland, 1990.
41. Soszko, M., J. Dłubak, and A. Czerwiński, *Quartz crystal microbalance study of palladium alloys. Part 1: Electrodeposition of Pt–Pd–Ru alloys*. Journal of Electroanalytical Chemistry, 2014. **729**: p. 27-33.
42. Schlesinger, M. and M. Paunovic, *Modern electroplating*. 2011: John Wiley & Sons.
43. Copland, E., *Partial thermodynamic properties of γ' -(Ni, Pt) 3Al in the Ni–Al–Pt system*. Journal of Phase Equilibria and Diffusion, 2007. **28**(1): p. 38-48.
44. Gaskell, D.R. and D.E. Laughlin, *Introduction to the Thermodynamics of Materials*. 2017: CRC press.
45. Yuan, K., et al. *Influence of Ru, Mo and Ir on the Behavior of Ni-Based MCrAlY Coatings in High Temperature Oxidation*. in *Turbo Expo: Power for Land, Sea, and Air*. 2014. American Society of Mechanical Engineers.
46. Sobolev, V., et al., *Development of substrate-coating adhesion in thermal spraying*. International materials reviews, 1997. **42**(3): p. 117-136.
47. Pawlowski, L., *The science and engineering of thermal spray coatings*. 2008: John Wiley & Sons.
48. Pukánszky, B. and E. Fekete, *Adhesion and surface modification*. Mineral Fillers in Thermoplastics I: Raw Materials and Processing, 1999: p. 109-153.
49. Wang, M.-J., S.-C. Chao, and S.-K. Yen, *Electrolytic calcium phosphate/zirconia composite coating on AZ91D magnesium alloy for enhancing corrosion resistance and bioactivity*. Corrosion Science, 2016. **104**: p. 47-60.

This is the accepted manuscript (postprint) of the following article:

Majid Hosseinzadeh, Erfan Salahinejad, *Comparative analysis of electrodeposited Pt, Ru and Pt-Ru overlays for high-temperature oxidation protection*, Surface and Coatings Technology, 496 (2025) 131685.

<https://doi.org/10.1016/j.surfcoat.2024.131685>

50. Yin, M., et al., *Thermodynamic properties, interfacial adhesion energy and tribological properties between MCN (M = Hf, Ta, Cr, Nb) coating and Ti alloy substrates investigated by experiment and first-principles calculations*. Applied Surface Science, 2024. **677**: p. 161068.
51. Young, D.J., *High temperature oxidation and corrosion of metals*. Vol. 1. 2008: Elsevier.
52. Sun, J., et al., *Microstructure and oxidation behaviour of Pt modified NiCrAlYSi coating on a Ni-based single crystal superalloy*. Surface and Coatings Technology, 2020. **399**: p. 126164.
53. Sohn, Y., et al., *Thermal cycling of EB-PVD/MCrAlY thermal barrier coatings: II. Evolution of photo-stimulated luminescence*. Surface and Coatings Technology, 2001. **146**: p. 102-109.
54. Slámečka, K., et al., *Thermal cycling damage in pre-oxidized plasma-sprayed MCrAlY+ YSZ thermal barrier coatings: Phenomenon of multiple parallel delamination of the TGO layer*. Surface and Coatings Technology, 2020. **384**: p. 125328.
55. Izumi, T., et al., *Effects of targeted γ -Ni+ γ' -Ni₃Al-based coating compositions on oxidation behavior*. Surface and Coatings Technology, 2007. **202**(4-7): p. 628-631.
56. Li, W., et al., *The role of Re in effecting isothermal oxidation behavior of β -(Ni, Pt) Al coating on a Ni-based single crystal superalloy*. Corrosion Science, 2020. **176**: p. 108892.